3D PiC Modelling of a experiment to investigate Auroral Kilometric Radiation Mechanisms

K.M. Gillespie[1], D.C. Speirs[1], S.L. McConville[1], K. Ronald[1], A.D.R. Phelps[1], A.W. Cross[1], C.W. Robertson[1], C.G. Whyte[1], R. Bingham[1,2], B.J. Kellett[2], I. Vorgul[3], and R.A. Cairns[3]

[1] *SUPA Department of Physics, University of Strathclyde, Glasgow, G4 ONG, Scotland.*
[2] *Space Physics Division, CCLRC, Rutherford Appleton Laboratory Didcot, OX11 0QX, England*
[3] *School of Mathematics and Statistics, University of St. Andrews, St. Andrews, KY16 9SS, Scotland*

A scaled laboratory experiment has been created to study the mechanism of Auroral Kilometric Radiation (AKR) generation which occurs naturally in the auroral zone of the Earth's magnetosphere. 3D PiC code simulations in KARAT were conducted to build on results from earlier 2D simulations and the measurements from the experiment. The 3D results proved to be consistent with results from the laboratory experiment, demonstrating coupling with modes having azimuthal structure which could not be analysed by the 2D simulations. Investigation is ongoing to study an up-shifted interaction regime, to investigate the viability of injecting a seed signal into the laboratory experiment and thus study spatial growth rate of the instability to compare with theoretical predictions.

1. Auroral Kilometric Radiation

Auroral Kilometric Radiation (AKR) is radio emission that occurs naturally above the Earth's ionosphere in the auroral zone at altitudes of around 1.5-3 Earth radii, centred around ~300kHz, with a peak power of 10^9W mainly polarised in the X-mode. It is produced in a large region of plasma depletion in the auroral zone, the auroral density cavity. It was first observed by Beneditkov as extra-terrestrial noise at around 1MHz [1]. AKR's properties were later characterised in 1980 by Gurnett and colleagues [2]. Similar emissions have been observed from other astrophysical objects [3]. The mechanism of AKR has been the subject of several conflicting theories. It is now thought that it is produced by a cyclotron maser instability in the descending electron flux. Several satellite missions have collected data from the AKR region [4-6]. Time resolved measurements of electron distribution functions within the AKR source region display a characteristic crescent shaped or horseshoe distribution. Such a horseshoe distribution is formed when a mainly rectilinear electron beam propagates into a region of increasing axial magnetic field and conservation of magnetic moment results in conversion of axial velocity $v_{//}$ into perpendicular velocity $v_\perp$ as the magnetic flux density increases [7].

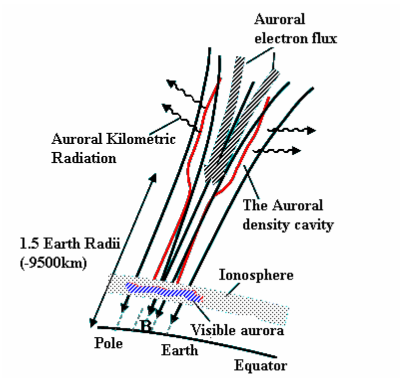

Figure 1: Illustration of AKR source region

2. Experimental Apparatus

A laboratory experiment was created to replicate the AKR generation process in a scaled geometry. The apparatus was scaled to microwave frequencies through a proportionally increased magnetic field. An electron beam injected from a velvet cathode by plasma flare emission was magnetically compressed by up to a factor of 17 and brought into resonance with the TE modes of an 8cm diameter cavity by a set of 6 DC magnet solenoids, Figure 2, which produced a convergent magnetic field reproducing the auroral geometry.

The beam is brought into resonance with near cut-off TE modes, as they have very similar polarisation

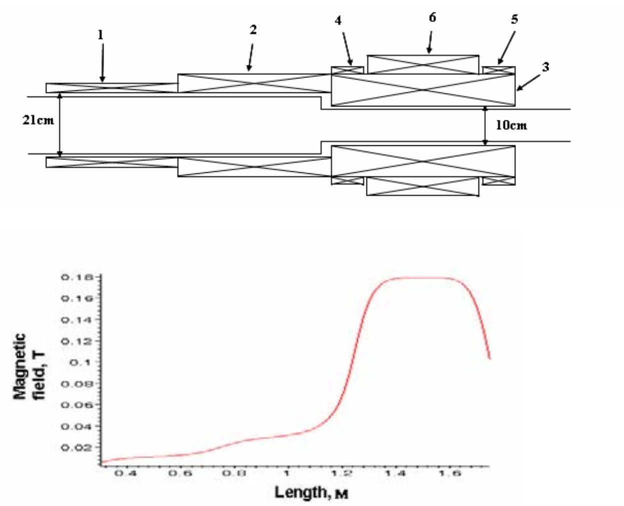

Figure 2: Experimental solenoid arrangement and magnetic field profile

and propagation properties to the X-mode. This experimental apparatus, formed a horseshoe distribution in the electron beam velocity space, comparable to that observed by satellite data.[8]

3. Two Dimensional Numerical Simulations

In order to simulate the experiment the 2D PiC code KARAT was used. The code was programmed with the dimensions of the vacuum vessel along with the magnetic field configuration. The simulation geometry is illustrated in Figure 3.

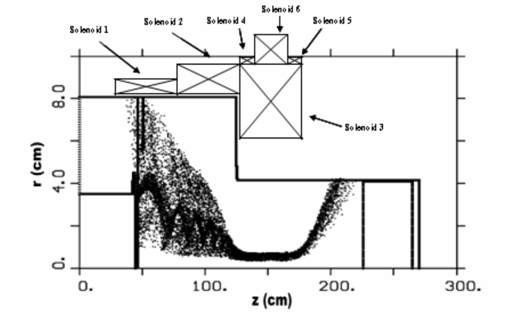

Figure 3: 2D Simulation of the experiment in KARAT showing the electron beam trajectory.

Two regimes of microwave resonance were studied at the magnetic field plateaux of B=0.48T and 0.18T, resonant with the $TE_{0,1}$ and $TE_{0,3}$ modes respectively. Results from the 2D simulations confirmed coupling to the $TE_{0,3}$ at a frequency of 11.7GHz, and the $TE_{0,1}$ mode at 4.45GHz corresponding to the two magnetic plateaux.

Peak output power was around 20kW at 11.7GHz, corresponding to an emission efficiency of ~1.3%. At 4.45GHz the output power was 25kW with efficiency ~2%.

Figure 4 illustrates the transverse against axial velocity of the beam which shows the horseshoe distribution formed at the entrance at the resonant section. [9]

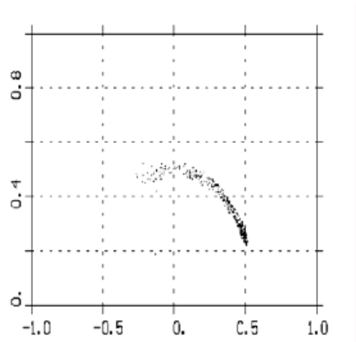

Figure 4: Phase space plot illustrating the horseshoe distribution.

4. Experimental results

The output spectrum from the experiment is shown in Figure 5 for the 4.45GHz and 11.7GHz resonances respectively.

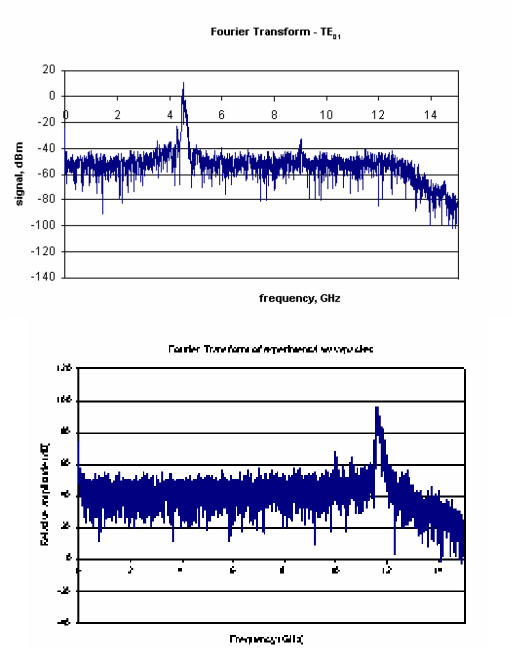

Figure 5: Spectrum of the output signal for (a) 4.45GHz and (b) 11.7GHz resonances.

It can be seen for both interactions there are other spectral components present. These modes were not predicted by 2D simulations due to the fact that modes with azimuthal were not accounted for.

5. Three Dimensional Numerical Simulations

Both the 4.45GHz and the 11.7GHz interaction regimes were simulated. The geometry and electron trajectories for the 3D simulations are shown in Figure 6(a). Figure 6(b) illustrates the mode structure produced from an axial view of the interaction regime at a resonant frequency of 4.45GHz.

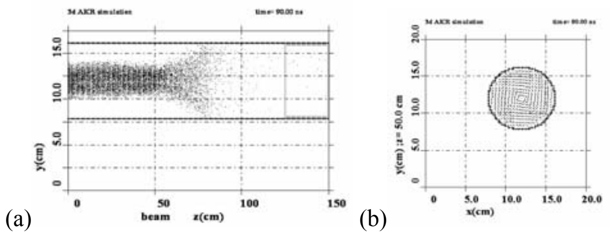

Figure 6: (a) Simulation geometry (b) Electric field mode structure.

Spectral analysis for the 4.45GHz 3D simulations confirmed the results of the 2D simulations, Figure 7. They also observed the 9GHz 2nd harmonic component measured experimentally.

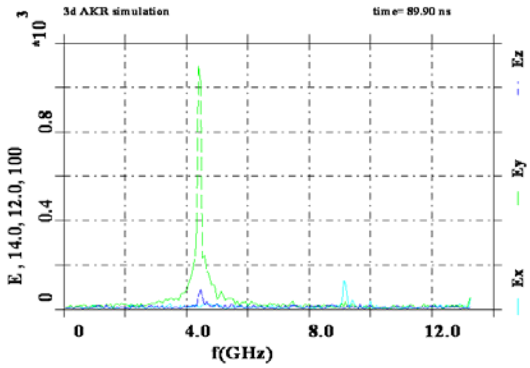

Figure 7: Spectra of RF emission from the electron beam at 4.45GHz resonance.

Peak RF power output at 11.7GHz resonance was found to be around ~17kW corresponding to efficiency of ~1%, comparable with the 2D simulations and experiments, Figure 8.

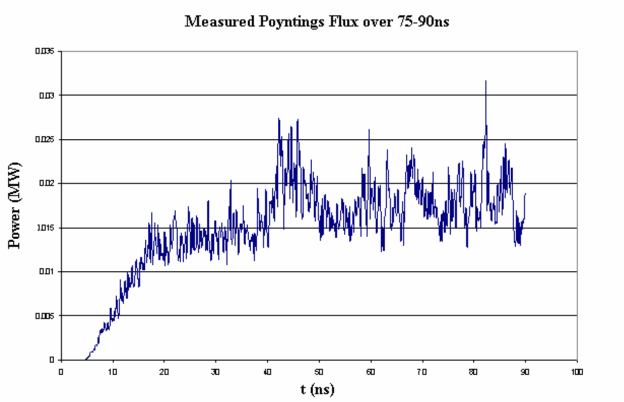

Figure 8: Output power at 11.7GHz

RF spectral output at the 11.7GHz resonance in Figure 9 showed a spectrum from 11.7GHz to 12GHz. Analysis indicated strong presence of the $TE_{2,3}$ mode as well as the expected $TE_{0,3}$ mode. This mode would not have been accounted for in 2D simulations as it has azimuthal structure.

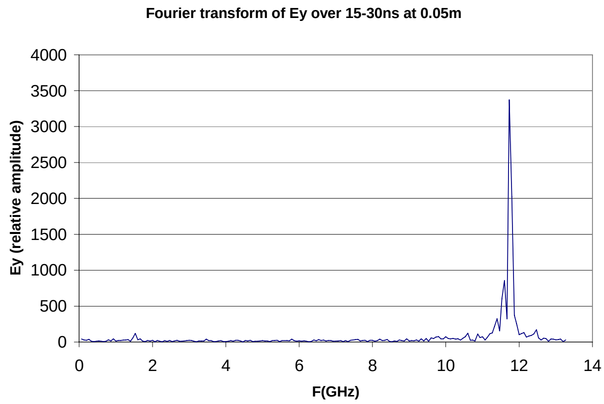

Figure 9: Spectra of RF emission for 11.7GHz.

6. Summary and Future work

3D PiC codes have been used to successfully reproduce the interaction between a complex electron beam and electromagnetic radiation. These new simulations have proven accurate in identifing the modes which were excited in the experiment. This work is leading to deeper understanding of the mechanism of auroral kilometric radiation emission. Future work will concentrate on study of the spatial growth rate of the instability.

7. Acknowledgments

This work was supported by the EPSRC. The authors would like to thank Mr I.S Dinwoodie for his help in creating the apparatus and Prof V.L Tarakanov for his assistance with the numerical codes.

8. References

[1] Wu C.S. and Lee L.C., J. Geophys. Res., **103**, (1998) 20159-20194.

[2] Gurnett D.A., J. Geophys. Res., **79**, (1974) 4227-4238.

[3] Kurth W.S., Nature, **433**, (2005) 722-725.

[4] Sato A. et al, Geophys. Res. Lett., **29** (2002), 2041.

[5] Roux A. et al, J. Geophys. Res., **98** (1993) 11657-11670.

[6] Gurnett D.A. et al, Annales Geophysicae (2001) 1259-1272.

[7] Bingham R, and Cairns R.A, Physics of Plasmas, **7** (2000) 3089-3092.

[8] Phelps A.D.R. et al, Proceeding of XXVIIth ICPIG, (2005) Eindhoven, the Netherlands.

[9] Speirs D.C., Ph.D. thesis, University of Strathclyde (2005)